

Joule heating effect in carbon-based epoxy resin: an experimental and numerical study

G. Spinelli^{1,2}, R. Guarini², R. Kotsilkova², E. Ivanov^{2,3*}, L. Vertuccio⁴, V. Romano⁵, L. Guadagno⁵

¹University of Study "Giustino Fortunato", Via Raffaele Delcogliano 12, 82100, Benevento, Italy

²Institute of Mechanics, Bulgarian Academy of Sciences, Acad. G. Bonchev Str., Bl. 4, 1113, Sofia, Bulgaria

³Research and Development of Nanomaterials and Nanotechnologies, NanoTech Lab Ltd., Acad. G. Bonchev Str., Bl. 4, 1113 Sofia, Bulgaria

⁴Department of Engineering, University of Campania "Luigi Vanvitelli", Via Roma 29, 81031 Aversa, Italy

⁵Department of Industrial Engineering, University of Salerno, Via Giovanni Paolo II, 84084 Fisciano (SA) Italy

Received: May 14, 2023; Revised: July 20, 2023

Extruded metals are the most common materials used for the production of heat sinks for thermal management. Nowadays, in the structural design phase, reduction of mass with consequent savings in materials and costs is one of the main aspects to consider. More recently, polymer-based nanocomposites with improved electrical and thermal properties are increasingly assessed for heat transport applications. The present study is focused on nanocomposites based on a structural epoxy resin filled with multi-walled carbon nanotubes (MWCNTs) which are prepared and then experimentally characterized. More specifically, after a preliminary investigation in terms of electrical conductivity, the temperature increase over time, due to the Joule heating effect is analyzed in response to different voltage values (70V, 80V, and 90V) applied to the test samples with a filler concentration of 3 wt%. These experimental results are used to validate a 3-dimensional numerical simulation carried out by using a commercial software (COMSOL Multiphysics®). A very positive agreement between experimental and modeling data is found. Once the model was validated, a number of physical properties of such nanocomposites related to the Joule heating were numerically explored for testing their potential practical use as heat exchangers. The aim of this study is to encourage the application of modern computational methods in conjunction with experimental techniques for adding knowledge in materials science. With this approach, new materials can be discovered or those already existing can be better investigated.

Keywords: carbon-based epoxy nanocomposites, thermal transport properties, multiphysics simulations, Joule-heating, electrical properties

INTRODUCTION

Low thermal and electrical properties are limitations not yet completely overcome when it comes to polymer-based composites, which are therefore classically recognized as insulating materials. Nevertheless, the use of polymers in thermal applications like heat exchangers is increasingly investigated for a series of benefits. Lightness, easy workability, cost reduction are just some of the remarkable properties compared to similar devices classically made by extrusion of metals, primarily aluminum and copper, which are high-density materials and, in particular, non-biodegradable [1, 2]. Recently, to achieve these goals, academic and industrial research efforts have been successfully focused to improve the overall electrical, mechanical and thermal properties of nanocomposites through the use of nanoscale fillers [3-6]. Among these nanofillers, carbon-based particles such as graphene and its derivatives, as well as carbon nanofibers (CNFs) and carbon nanotubes (CNTs), have attracted great attention, owing to their

excellent intrinsic physical properties and their strong interfacial interactions, when dispersed in the host polymer matrices [7]. In particular, since the discovery of their existence, CNTs have been widely considered as promising fillers for developing new advanced polymer nanocomposites due to their chemical stability (their carbon atoms form sp² covalent bonds with honeycomb structure), their unique 1-dimension geometry and their large aspect ratio. All these peculiar characteristics are suitable to form percolation paths which support the electrical and thermal transport within the polymer, thus enhancing the general physical properties of the resulting materials. Smoleń *et al.* have investigated the effect of multiwalled carbon nanotubes produced by catalytic chemical vapor deposition and then subjected to covalent functionalization, on the mechanical and electrical properties of epoxy-based composites in which the percolation threshold was obtained with 1 wt% addition of filler [8]. The use of a surfactant (Triton X-100) to enhance the dispersion state of carbon nanotubes in epoxy polymers for improving the thermomechanical, mechanical and

* To whom all correspondence should be sent:
E-mail: ivanov_evgeni@yahoo.com

electrical properties of the resulting nanocomposites was evaluated by Geng *et al.* [9].

Moreover, mechanical processing methods based on a high-pressure homogenizer and a three-roll calendaring mill in combination [10], were proposed to achieve a well dispersed nanofiller thus enhancing the toughness and electrical properties of the CNT-based epoxy composites which exhibit a low percolation threshold (about 0.01 wt%).

The adoption of carbon-based nanofillers for the development of epoxy-based vinyl ester composites with improved mechanical and electromagnetic properties were also considered in view to their potential use in aerospace applications as radar absorbing materials [11].

Thermally and electrically conductive epoxy nanocomposites including carbon nanotubes have been proposed for practical applications in electronics, automotive, and aerospace industries to dissipate heat or to avoid static charge [12].

In the present study, samples based on an epoxy resin filled with different filler content (0.3, 0.5, 1, 2 and 3 wt%) of multiwall carbon nanotubes (MWCNTs) were produced and then experimentally characterized. Based on the results of a preliminary electrical investigation, the electrically most conductive composite (epoxy containing 3 wt% of MWNTs) was selected for thermo-electric insights on the Joule effect due to different voltage values (70 V, 80 V and 90 V) applied to the samples. Joule heating was explored not only experimentally but

also through a simulation study carried out with a commercial software (COMSOL Multiphysics®). A good match between experimental and numerical results was found. This means that computational studies are welcomed in materials science to discover new materials and their properties, to better investigate the existing ones, to explain experimental results, to determine material behavior under specific conditions, mechanisms, theories and much more.

MATERIALS AND METHODS

In the present study, the nanocomposites for the experimental tests were manufactured by mixing up, in accordance with a procedure already described in Spinelli *et al.* [13], the following phases: i) an epoxy matrix 3,4-epoxycyclohexylmethyl-3',4'-epoxycyclohexane carboxylate (ECC) which serves as a precursor; ii) a curing agent based on methyl hexahydrophthalic anhydride (MHHPA); iii) multiwall carbon nanotubes (commercial name: Arkema Graphistrength® C100) as a conductive nanofiller. The above-mentioned constituents were suitably combined to obtain samples with different concentrations, i.e. [0.3, 0.5, 1, 2 and 3] wt%. The crucial physical and chemical characteristics of precursor, hardener agent and filler, as well as the size of the parallelepiped-shaped test specimens, are briefly summarized in Figure 1. More information can be found in Guadagno *et al.* [14].

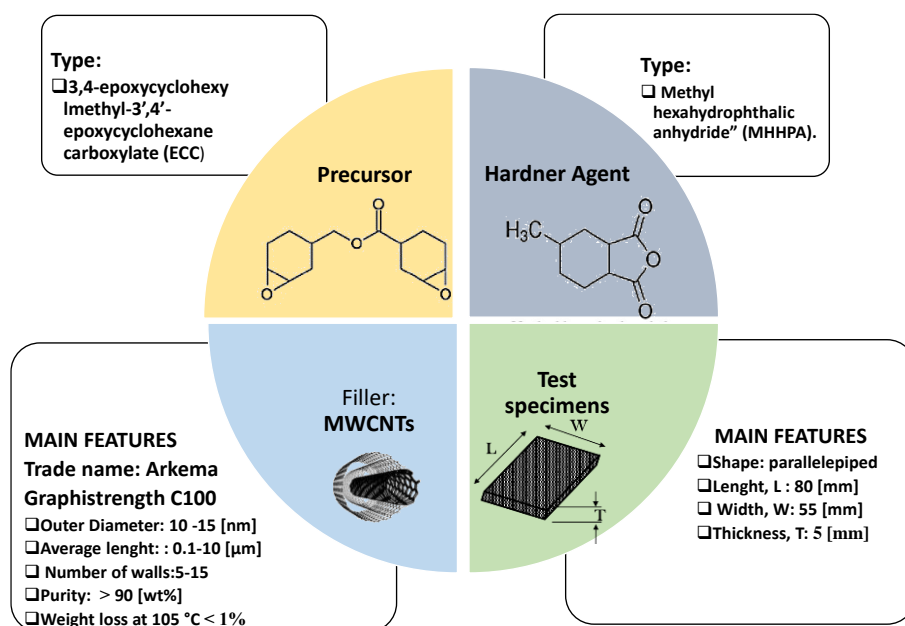


Figure 1. Principal characteristics of the phases of compounds and test samples.

Since the test specimen resistance is of the order of several kΩ, its electrical conductivity was evaluated with a two-probe measurement by assuming the contact resistance negligible, as successfully adopted in literature and in our previous studies [15-18]. On the basis of the results of this preliminary electrical characterization, the electrically most conductive composites containing 3 wt% CNTs have been selected for the experimental and numerical investigation of Joule heating effect.

For this aim, silver paint (commercial name: RS 196-3600) was placed on the short sides of the test samples to provide ohmic contacts between the power supply EA-PSI 8360-10T (Elektro-Automatik, 0–360 V, 0–10 A, 1 kW max) and the HP34401A ammeter (min current 0.1 μA). In particular, the variation over time of the top surface temperature of the specimens, due to Joule heating generated by different values of applied voltage (70V, 80V and 90V) was experimentally observed. These thermal profiles were monitored by means of a thermocouple from which the data were directly acquired by a data acquisition board (Data Logger TC-08 supplied by Pico Technology) managed with the respective software PicoLog. A schematically representation of this thermo-electric measurement setup is shown in Figure 2.

A numerical investigation of the Joule heating effect has been carried out through the software COMSOL Multiphysics®, which is based on Finite

Element Method (FEM). The results of the simulation study were then compared with the experimental ones. A schematic representation of the case study addressed in the present work and the main model definitions is reported in Figures 3a) and b), respectively.

With a reference to a differential volume $\Delta x \Delta y \Delta z$, the governing equation for heat transfer in a solid (at constant pressure) used in the numerical simulations can be expressed in cartesian coordinates, according to the following expression:

$$\frac{\partial}{\partial x} \left(\lambda \frac{\partial T}{\partial x} \right) + \frac{\partial}{\partial y} \left(\lambda \frac{\partial T}{\partial y} \right) + \frac{\partial}{\partial z} \left(\lambda \frac{\partial T}{\partial z} \right) + Q|_{Joule\ heating} = \rho c_p \frac{\partial T}{\partial t} \quad (1)$$

where λ , ρ and c_p are the thermal conductivity [$Wm^{-1}K^{-1}$], the density [kgm^{-3}] and the specific heat [$Jkg^{-1}K^{-1}$] of the material, respectively, whereas $Q=J \cdot E$ is the source term [Wm^{-3}] of the Joule heating related to the electric current. More in details, J represents the current density [Am^{-2}] and E is the electric field strength [$VA^{-1}m^{-1}$] generated by the different voltage values (70V, 80V, 90V). Table 1 summarizes the initial and boundary conditions for uniquely resolving the thermal balance of eq. (1).

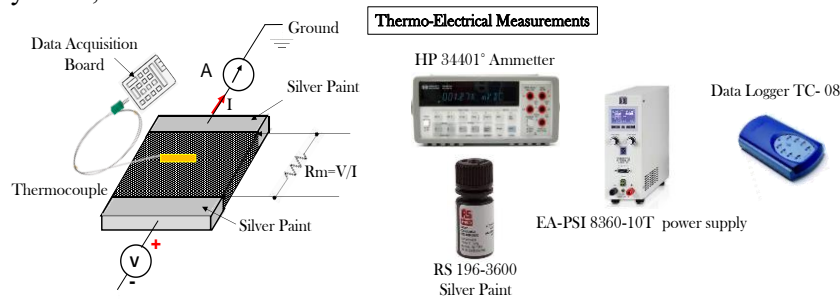


Figure 2. Schematic representation of the thermo-electric and Joule heating tests with the main adopted laboratory apparatus.

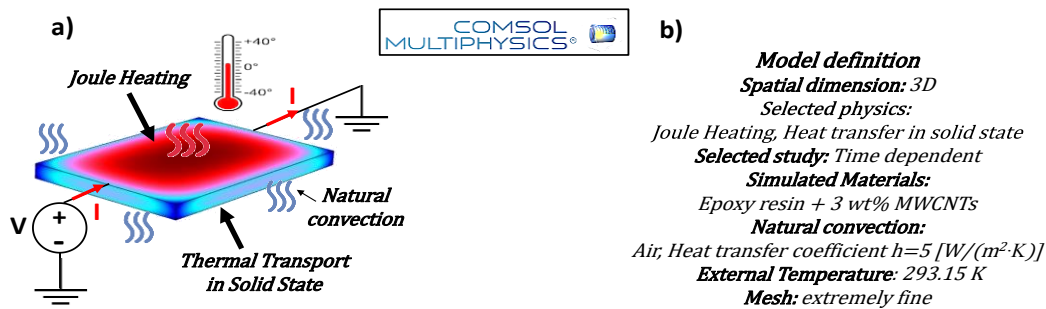


Figure 3. a) Case study addressed in the present study; b) Main model definitions for the numerical investigation adopted in COMSOL Multiphysics

Table 1. Initial and boundary conditions (I.C. and B.C., respectively) for resolving equation 1.

Initial (I.C.) and boundary (B.C.) conditions		Equations	Validity
I. C.	$t=0$	$T=\text{Room Temperature}$ (T_0)	$\forall x, \forall y, \forall z$
B. C.	<i>Upper and Lower Surfaces</i> $z=0$ $z=5$	$-\lambda \frac{\partial T}{\partial z} = h \cdot (T - T_\infty)$	$(\forall x, \forall y, t > 0)$
B. C.	<i>Lateral Surfaces</i> $y=0$ $y=55$	$-\lambda \frac{\partial T}{\partial y} = h \cdot (T - T_\infty)$	$(\forall x, \forall z, t > 0)$
B. C.	<i>Back and Front Surfaces</i> $x=0$ $x=80$	$-\lambda \frac{\partial T}{\partial x} = h \cdot (T - T_\infty)$	$(\forall y, \forall z, t > 0)$

RESULTS AND DISCUSSION

DC electrical characterization

As it is expected by the percolation theory, the trend of the electrical conductivity (σ_{DC}) exhibits a power law dependence, which is classically described by the following equation:

$$\sigma_{DC} = \sigma_0 \cdot (\nu - E.P.T.)^t \quad (2)$$

for $\nu > E.P.T.$

where the preexponential factor σ_0 , represents the intrinsic electrical conductivity of the nanofillers, ν is the instantaneous filler concentration and t is a critical exponent, which depends on the dispersion state of the filler within the matrix [19]. The term *E.P.T.* accounts for the well-known electrical percolation threshold, i.e. the minimum filler loading, at which the electrical behavior of the polymeric matrix changes from insulator to conductive, due to at least one established percolation path. Due to the good dispersion of the nanotubes and their ability to form the percolation network, this electrical threshold is achieved, in our

case, with the modest concentration of 0.3 wt%. With this amount of MWCNTs, the overall macroscopic electrical conductivity of the resulting nanocomposites is equal to $6.5 \cdot 10^{-3}$ S/m, whereas at the concentration of 3 wt% it is about $6.8 \cdot 10^{-2}$ S/m.

The latter formulation (epoxy+3wt% of MWCNTs), being the most conductive among those investigated in the present study, is therefore adopted to both experimental and numerical analysis of the thermal properties due to Joule heating effect.

Figure 4 a) shows the so-called percolation curve, i.e. the variation of the electrical conductivity as function of the filler concentration, for the nanocomposites investigated in the present study. Moreover, as commonly verified in literature [20-22] and as shown in Fig. 4b), a theoretical investigation, confirming that the tunneling effect is the main electrical conduction mechanism in composite materials is the existence of a linear correlation between the electrical conductivity (expressed in natural logarithmic) as function of $\nu^{-1/3}$. The value of the coefficient of determination R^2 close to 1 confirms the validity of this assumption.

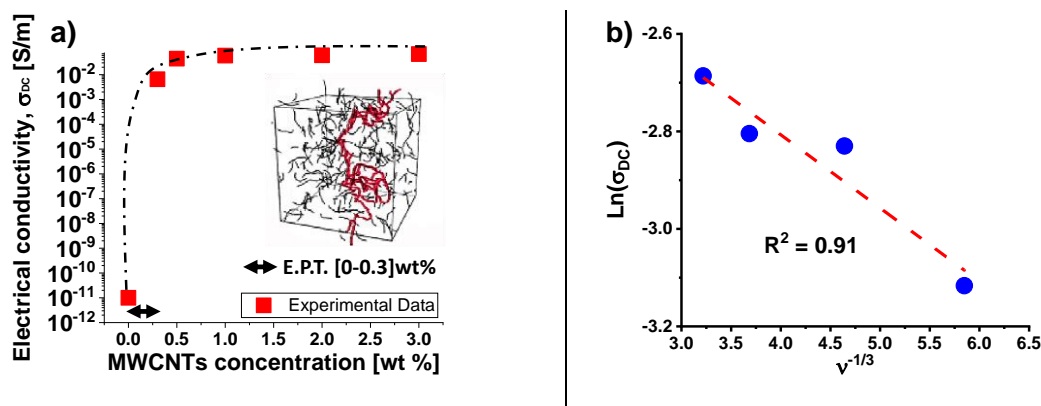


Figure 4. a) Percolation-curve for the epoxy-based nanocomposites filled with different filler concentrations; b) Statistical approach, confirming the role of electron tunneling as the main conduction mechanism in composite materials.

Experimental results on Joule heating effect

Figure 5 a) presents the experimental trend of the upper surface temperature over the time (up to 3600 s), when three different voltage values (70, 80 and 90 V) are applied to the test specimens including 3 wt% of MWCNTs.

From a physical point of view, it is possible to note how the heat transfer begins as transient and then reaches a steady-state, when a thermal equilibrium is reached. More in details, during the transient heat transfer, when the heat flow rate keeps changing, the temperature of the medium is a function of time, $T = T(t)$ for a short duration (t^* denoted in the figure). It rises quickly and exponentially tends toward constant steady-state values (indicatively 324K, 331K and 338K, at 70V, 80V, 90V, respectively). A magnification of such time windows is reported in Figure 5b).

During the steady-state transfer which is characterized by a constant and specific rate of heat transfer, the temperature is constant throughout time. This is because the total amount of heat transfer due to the Joule heating is equal to that dissipated with the surrounding area through natural convection. In particular, as shown in Figure 5c), these steady-state values (at $t=3600$ s) are linearly proportional (the coefficient of determination R^2 is strictly close to 1) to the applied voltage values.

This result is in line with the theoretical prediction since the Joule effect, analytically equivalent to a thermal power dissipation P , depends linearly on the voltage V , according to the relation $P=V \cdot I$ where I is the electrical current. Differently, as shown in Figure 5 d), a near-perfect exponential fit (otherwise, a coefficient of determination equal to 0.973 is found with a linear fit or equal to 0.981 with a power-law fit) is found for the experimental data concerning the heat rate, HR [$Kmin^{-1}$] as a function of the applied voltage. For reasons of clarity, the heat rates are calculated as slopes of the corresponding curves (S_{90V} , S_{80V} and S_{70V}) of Figure 5b) during the first instants of the transient phase.

Numerical study on Joule heating effect

Computational studies involving simulations, modeling and theoretical approaches are increasingly used for developing new materials and to better explain the properties of existing ones.

Figure 6 illustrates the electric potential distribution (left part) and the 3D temperature profiles (right part) by simulating, in a finite element software, the nanocomposites based on 3 wt% of MWCNTs, when subjected to the three different voltage values, as it was the case for the experimental measurements (70, 80 and 90 V in Figs. 6 a), b) and c), respectively).

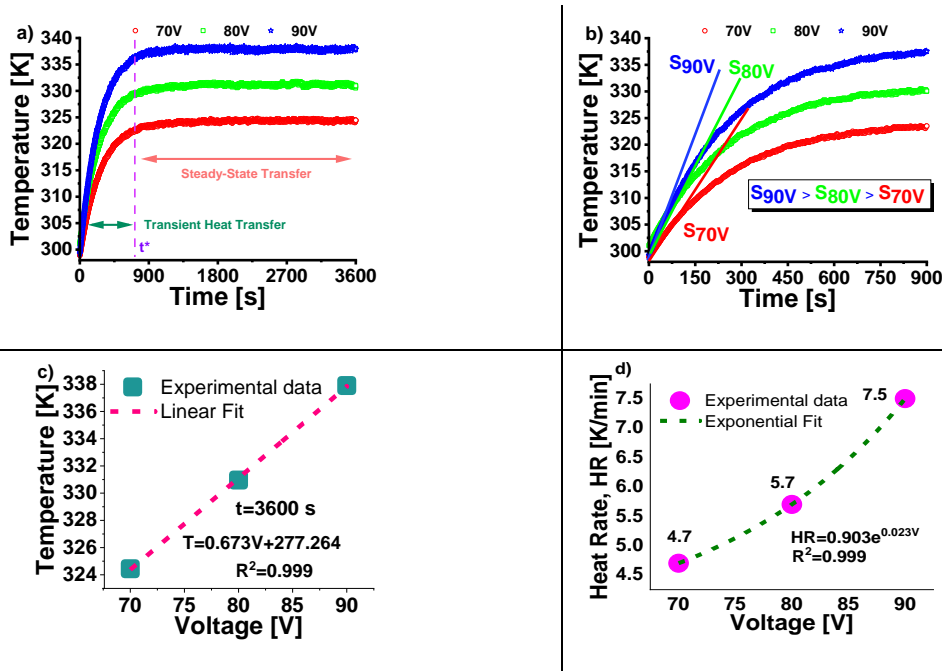


Figure 5. a) Temperature profiles due to Joule heating at different applied voltage values (70, 80 and 90 V); b) Magnification of the transient heat transfer time windows; experimental and curve fitting of the steady-state temperature values and heat rate as function of the voltage levels in c) and d), respectively.

It is worth noting that the electrical potential linearly increases along the increasing x- axis and therefore, it was found that the position of the minimum and maximum electric potential strength occurred at the position 0 mm and 8 mm, respectively, along the direction to which the voltage is applied. As it is expected, it assumes constant values in each transversal cross-section.

Even more interestingly is that almost the same steady-state values for the surface temperatures are numerically found (see the color bars: 323K, 331K and 339K at 70V, 80V, 90V, respectively) by means the multiphysics simulations, thus confirming an interesting agreement between experimental and numerical results.

The use of a 3D software representation allows to graphically explore the temperature distribution on the solid and identify the hottest areas (central parts), compared to those less heated (edges and corners).

In order to deepen this investigation, Figure 7 shows the simulated convective heat flux (at t= 3600 s) for the simulated nanocomposite, always distinguished according to the voltage level applied (70, 80 and 90 V in a), b) and c), respectively). First of all, as evident from the analysis of these figures, the convective flux is visibly greater on the larger surfaces of the sample, than on the lateral ones, since this main mode of thermal energy transport directly depends on the exchange area (and also on the higher temperature achieved in this region) in agreement with Newton's law of cooling, analytically expressed by the following relation:

$$Q = h \cdot S \cdot \Delta T$$

where h [W/m²·K⁻¹] is the heat transfer coefficient by natural convection, that denotes the proportionality term between the heat flow Q [W] and the temperature difference ΔT [K], which origins the convective transport between a hot solid surface S [m²] and the surrounding air. Moreover, by referring to such graphics with their relative color bars it is also possible not only to quantify these heat fluxes but also to evaluate the different rates (the greater the applied voltage, the greater is the temperature difference and consequently the convective flux).

To conclude such numerical investigation, Figure 8 shows the 3D views of the total internal energy U (at t=3600 s) for the nanocomposite, when it undergoes a voltage test of 70, 80 and 90V, in a), b) and c), left part, respectively. Instead, in the corresponding right-hand parts of the same Figure 8 are shown the two-dimensional graphics of this state variable U , as a function of the length [mm] in correspondence of the symmetry axis along the x-direction. The choice to report the view of some selected cross-section of the sample is driven by the opportunity to show a visual inspection of its change in all spatial directions.

Before discussion of the numerical results, it is important to recall that the internal energy of a solid depends on temperature, i.e. $U=U(T)$ and in particular that its variations ΔU can be expressed in the simple form:

$$\Delta U = U(T_f) - U(T_i) \quad (4)$$

where T_f and T_i indicate the initial and final temperature of the solid, respectively.

By convention it is assumed that if $\Delta U >0$, the solid absorbs heat from the outside: this implies that, consequently, the thermal agitation of the constituent atoms increases. Otherwise, if $\Delta U <0$, the solid transfers its heat outside by cooling thus reducing its atomic vibrations. As is clearly visible from Figure 8, our simulation study is in agreement with such theoretical aspects. First of all, the internal energy is positive since the sample is warming up due to the Joule effect, i.e. due to the current that flows in it, as a consequence of the applied voltage which in turn affects the rate of this internal energy variation (higher the voltage, greater the rate). Moreover, due to the key role that the temperature plays in determining such changes, the internal energy U appears visibly uneven throughout the sample given its non-uniform local heating. As is better evident from the bidimensional graphics, the total internal energy varies parabolically along the length in the x-axis direction (as is the case of the temperature profile, unless a scaling factor corresponds to the specific heat), to reach a maximum at the center of the sample (at x=40 mm) and minimum values in the terminal parts (x=0 mm and x= 80 mm), which are decisively colder, as previously discussed.

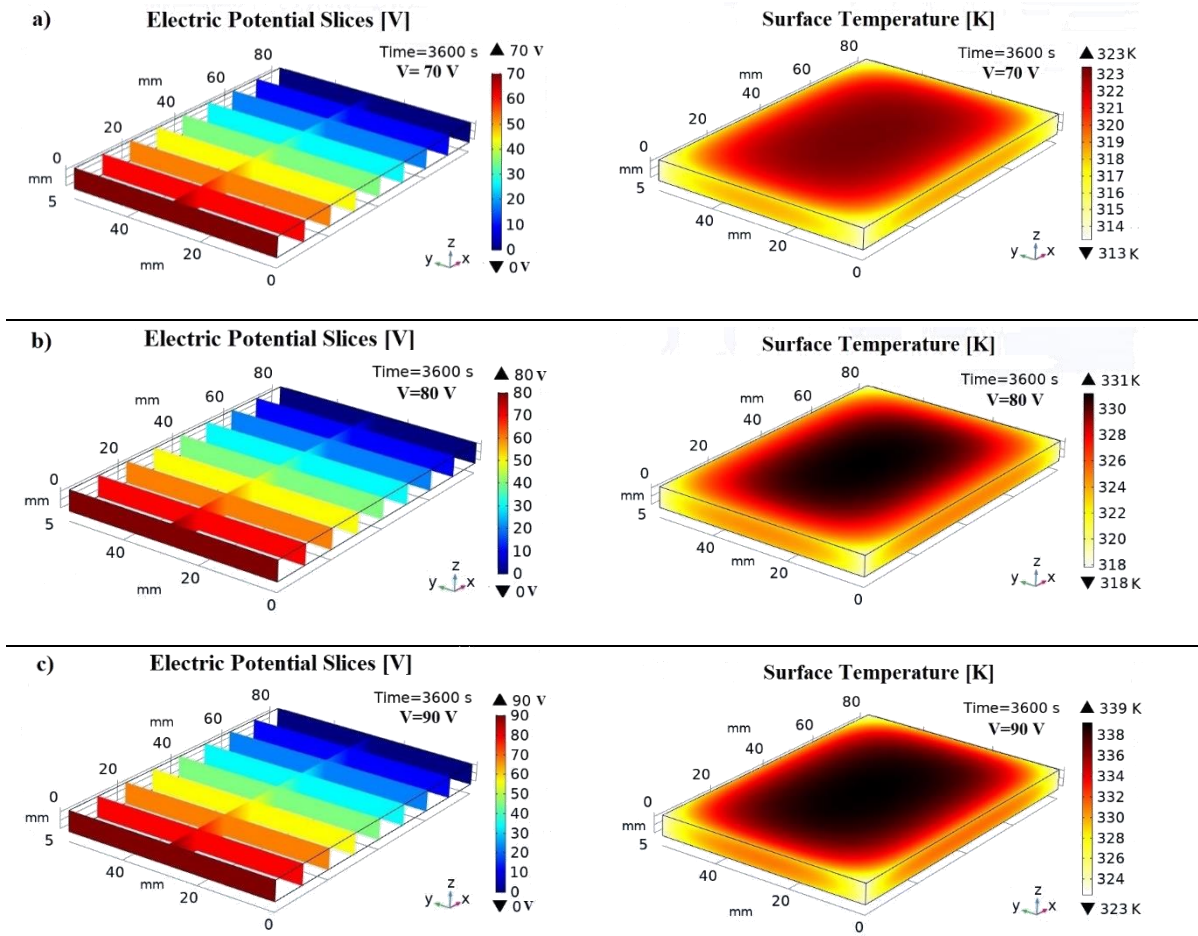


Figure 6. Electric potential distribution (left part) at $t=3600$ s along the direction to which the different voltage (70V, 80V and 90V, in a), b) and c), respectively) is applied. In the right part, the graphics show the 3D views of the corresponding surface temperature reached by Joule effect.

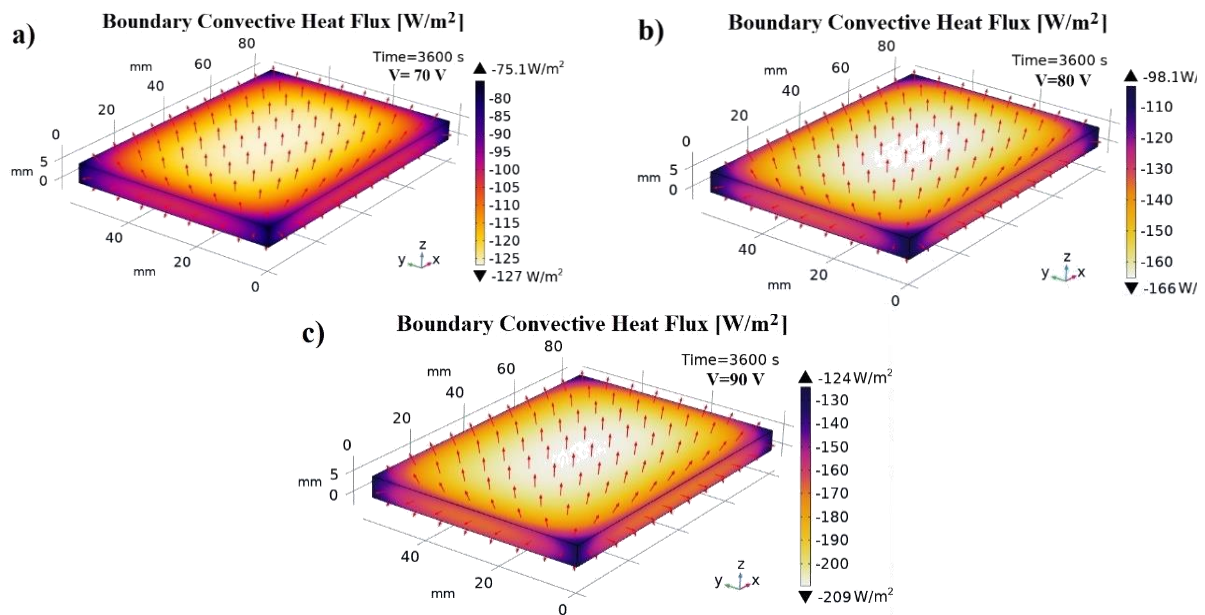


Figure 7. Convective flux at $t=3600$ s in case of applied voltage of 70, 80 and 90V in a), b) and c), respectively.

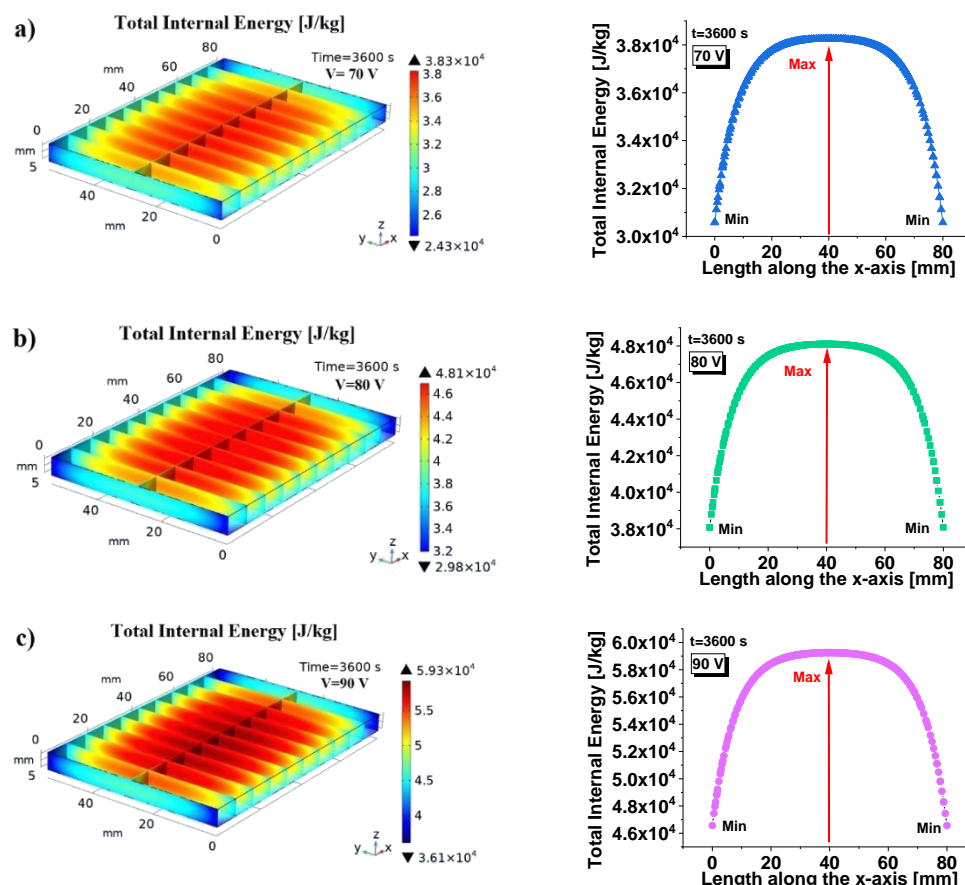


Figure 8. 3D-views (left part) of the total internal energy at $t=3600$ s due to the Joule heating effect, as a consequence of the different voltage values, 70V, 80V and 90V, applied to the sample in a) b) and c), respectively. In the right part, the graphics show the corresponding total internal energy as a function of the length in the x-axis direction.

CONCLUSION

Thermoelectric behavior of epoxy resin filled with 3 wt% of MWCNTs, due to Joule heating effect, was experimentally and numerically investigated. In particular, different thermal aspects, due to the Joule heating effect, when different voltage values (70 V, 80 V and 90 V) were applied to the samples, were numerically analyzed by means of a simulation study performed with a commercial software (COMSOL Multiphysics®). Given the good agreement found between experimental and simulation results, numerical studies by application of innovative computational approaches are encouraged in material science to design and to manufacture new advanced materials or to better investigate and optimize the existing ones. Further thermal aspects will be investigated in a future paper to explore the potential use of electrically and thermally conductive polymers in practical thermal applications such as heat exchangers.

Acknowledgements: This research was supported by the project BG05 M2OP001-1.001-0008 “National Center for Mechatronics and Clean

Technologies” of Republic of Bulgaria and by the H2020-FET-Graphene Flagship-881603 Graphene Core 3. The authors would like to acknowledge the EU Horizon 2020 RISE Project ReACTIVE Too (Grant Agreement No 871163).

REFERENCES

1. J. Mark, K. Ngai, W. Graessley, L. Mandelkern, E. Samulski, G. Wignall, J. Koenig, Physical properties of polymers, Cambridge University Press, Cambridge, 2004.
2. H. Zhang, T. Shi, A. Ma, *Polymers*, **13**, 2797 (2021).
3. G. Spinelli, R. Guarini, R. Kotsilkova, E. Ivanov, V. Romano, *Nanomaterials*, **11**, 1511 (2021).
4. G. Spinelli, R. Guarini, R. Kotsilkova, T. Batakliiev, E. Ivanov, V. Romano, *Materials*, **5**, 986 (2022).
5. R. Kotsilkova, E. Ivanov, V. Georgiev, R. Ivanova, D. Menseidov, T. Batakliiev, V. Angelov, H. Xia, Y. Chen, D. Bychanok, P. Kuzhir, R. Di Maio, C. Silvestre, S. Cimmino, *Polymers*, **12**, 1208 (2020).
6. E. Ivanov, R. Kotsilkova, H. Xia, Y. Chen, R. K. Donato, K. Donato, A.P. Godoy, R. Di Maio, C. Silvestre, S. Cimmino, V. Angelov, *Appl. Sci.*, **9**, 1209 (2019).
7. C. I. Idumah, C. M. Obele, *Surf. Interfaces*, **22**, 100879 (2021).

8. P. Smoleń, T. Czujko, Z. Komorek, D. Grochala, A. Rutkowska, M. Osiewicz-Powężka, *Materials*, **14**, 3325 (2021).
9. Y. Geng, M. Y. Liu, J. Li, X. M. Shi, J. K. Kim. *Compos. Part A Appl.*, **39**, 1876 (2008).
10. R. Hollertz, S. Chatterjee, H. Gutmann, T. Geiger, F. A. Nüesch, B.T.T. Chu, *Nanotechnology*, **22**, 125702 (2011).
11. F. Marra, A.G. D'Aloia, A. Tamburrano, I.M. Ochando, G. De Bellis, G. Ellis, M.S. Sarto. *Polymers*, **8**, 272 (2016).
12. A. Moisala, Q. Li, I. A. Kinloch, A. H. Windle, *Compos. Sci. Techn.*, **66**, 1285 (2006).
13. G. Spinelli, P. Lamberti, V. Tucci, L. Guadagno, L. Vertuccio, *Nanomaterials*, **10**, 434 (2020).
14. L. Guadagno, R. Longo, F. Aliberti, P. Lamberti, V. Tucci, R. Pantani, G. Spinelli, M. Catauro, L. Vertuccio, *Nanomaterials*, **13**, 495 (2023).
15. G. Spinelli, R. Kotsilkova, E. Ivanov, V. Georgiev, R. Ivanova, C. Naddeo, V. Romano, *Polymers*, **12**, 2414 (2020).
16. L. Vertuccio, L. Guadagno, G. Spinelli, P. Lamberti, V. Tucci, S. Russo, *Compos. B. Eng.*, **107**, 192 (2016).
17. J. Ku-Herrera, F. Avilés, *Carbon*, **50**, 2592 (2012).
18. A. Oliva-Avilés, F. Avilés, V. Sosa, *Carbon*, **49**, 2989 (2011).
19. C. W. Nan, Y. Shen, J. Ma, *Annu. Rev. Mater. Res.*, **40**, 131 (2010).
20. M. T. Connor, S. Roy, T. A. Ezquerra, F. J. B. Calleja, *Phys. Rev. B*, **57**, 2286 (1998).
21. A. Mdarhri, F. Carmona, C. Brosseau, P. Delhaes, *J. Appl. Phys.*, **103**, 054303 (2008).
22. B. E. Kilbride, J. Coleman, J. Fraysse, P. Fournet, M. Cadek, A. Drury, S. Hutzler, S. Roth, J. W. Blau, *J. Appl. Phys.*, **92**, 4024 (2002).